Heliyon 10 (2024) e25142

Contents lists available at ScienceDirect

Heliyon

journal homepage: www.cell.com/heliyon

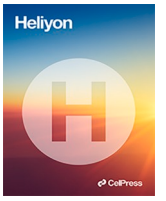

Research article

Experimental study on the effect of quaternary ammonium salt + monoethylene glycol compound to methane hydrate agglomeration in oil-water system

Qibin Zhao [a,*], Hao Liang [b]

[a] Exploration and Development Department, CNOOC, Beijing, China
[b] Exploration and Development Department, Hainan Branch of CNOOC, Haikou, Hainan, China

ARTICLE INFO

Keywords:
Quaternary ammonium salt
MEG
Methane hydrate
Anti-agglomerating
Oil-water system

ABSTRACT

Natural gas hydrate has been a critical risk to the safety of offshore oil and gas well test and subsea transportation. Herein, the effect of three quaternary ammonium salt (QAS) surfactants with monoethylene glycol (MEG) to methane hydrate agglomeration in water-oil system was experimentally studied by a rocking cell. Based on the hydrate volume fraction and the slider trajectory, a classification method of the gas hydrate anti-agglomerants was established. All the QASs in this work show the capability of reducing hydrate agglomeration, among which N^1,N^3-didodecyl-N^1,N^1,N^3,N^3-tetramethylpropane-1,3-diaminium chloride (AA-2) has the best anti-agglomerating performance, and the slider moved at a large trajectory of 61–174 mm. The three QASs were compounded with 5, 10, and 15 wt% (based on water) MEG, respectively. Experimental results showed that AA-2 compounded with MEG (10 wt%) can effectively prevent hydrate agglomeration. The slider moved in the cell at the full trajectory range, showing the compound of grade A performance. The compound of QAS and MEG shows a synergistic effect. The addition of QAS can significantly reduce the required MEG dosage for the hydrate blockage prevention than the MEG only situation. Considering the economic factors of the filed hydrate management, the combination application of QAS + MEG may provide a promising option.

1. Introduction

Natural gas hydrate (NGH) is a non-stoichiometric crystal substance in which gas molecules are trapped in the water molecule formed cages [1]. Common components in natural gas such as methane and ethane could form gas hydrate at the favorable temperature and pressure. At present, three types of NGH structure (sI, sII and sH) have been identified in natural NGH reservoirs as well as oil/gas industries [2]. During the offshore oil and gas transportation and production, the high pressure and cold environment at the seabed makes it easy for hydrate formation in the wellbores, pipelines or other facilities [2]. The formation and agglomeration of NGH occurring in subsea facilities might induce critical risk for the safety of production or transportation, and cause significant economic losses [2]. Therefore, natural gas hydrate has been one of the biggest menaces for the flow safety in the offshore oil and gas industries [3].

Based on the formation principles of NGH plugs, dehydration, depressurization, heating or chemical injections could prevent the

* Corresponding author.
E-mail address: zhaoqb@cnooc.com.cn (Q. Zhao).

https://doi.org/10.1016/j.heliyon.2024.e25142
Received 13 August 2023; Received in revised form 13 January 2024; Accepted 22 January 2024
Available online 26 January 2024

hydrate plugging [4]. However, dehydration could not be used until the stream reach the platform. Depressurization and heating methods are usually limited by the operating conditions of the subsea facilities. Therefore, chemical injection strategies have been widely employed in the field [2,5]. Chemicals for hydrate management could be classified into thermodynamic hydrate inhibitors (THIs), kinetic hydrate inhibitors (KHIs), and anti-agglomerants (AAs) [6]. Among the chemicals, THIs change the phase equilibrium conditions of gas hydrate, shifting the NGH phase boundary to a tough P-T region for formation [1]. KHIs inhibit the hydrate crystals nucleation or delay the hydrate crystal growth [1,6,7]. However, the KHIs may fail to be applied in the extreme subcooling situations (>10 °C). Hydrate AAs are capable of inhibiting the NGH particle agglomeration by adsorbing on the NGH crystal surface, so that the well dispersion or suspension of NGH particles could be achieved in the continuous fluid (oil, water or gas) [6]. However, the application of hydrate AAs requires sufficient liquid volume in the system to form the transportable hydrate slurry. In some cases, the performance of hydrate AAs also exhibited strong dependence on the water cut in pipes. The performance of hydrate AAs may be limited with the variation of the water cut, [8,9]. KHIs and AAs are called Low Dosage Hydrate Inhibitors (LDHIs), due to the much lower dosage (<3 wt% with regard to water) compared with THIs (20–60 wt%). THIs are considered to be a more reliable in hydrate avoidance but the cost is high, while LDHIs are effective at low dosage but with less reliability than THIs. Therefore, the combination of LDHIs and THIs may be a potential choice for the efficient and reliable prevention of hydrate blockage.

To solve the NGH blockage problems, the exploration of efficient hydrate AAs has raised great interests, which can be applied for the NGH management in deep-sea high subcooling environment. Quaternary ammonium salts (QASs) are representative AAs which were firstly reported in 1993 [10]. Since then, the performance of QAS on NGH particle anti-agglomeration in various situations was verified by many researchers [11–15]. Delroisse et al. [11] investigated the anti-agglomerating behavior of QAS using cyclopentane or methane/propane as former by microscopic observation of NGH morphology. Results showed that QAS can effectively reduce the hydrate agglomeration. During their follow-up research, the effectiveness of QAS on NGH anti-agglomeration was further confirmed [16]. Recently, some hydrate AAs with good biodegradability have been developed for the environmental consideration [8,17–20]. Yan et al. [20] revealed the rheological characteristics of the NGH slurry in the flow loop, which involved plant-extracted AAs. Analysis indicated that the NGH slurry could easily and safely flow upon launching from the static condition of the shutting-down situation using the proposed AAs. Subsequently, Wang et al. [19] determined the main active components of the hydrate AAs as luteolin and apigenin using the stirring cell. Sun and Firoozabadi [21] proposed a nonionic AA which could minimize the NGH agglomeration regardless of the water content range in pipes. Follow-up investigations showed that the capability of hydrate AAs could be improved by compounding the hydrate AA with salt, alcohol or Span 80 [22–24]. At the water cut of 20 %, the minimum effective AA concentration can be lowered from 1 wt% to 0.6 wt% after adding the salt. At the water cut range of 10 wt%, synergistic inhibition effect of Span 80 and AA on NGH agglomeration was observed, and the agglomeration of hydrate can be prevented by using 0.25 wt% AA + 0.75 wt% Span 80. At the high water cut of 95 %, the presence of alcohols is capable of inhibiting the flocculation of emulsion with very high viscosity.

In the past few decades, the combination application of LDHIs and THIs has been investigated. Foroutan et al. [25] compared the synergistic effect of polyethylene glycol (PEG) with the different molecular weights on the inhibition capability of commercial KHIs (PVP and Luvicap EG). Results showed that PEG of the larger molecular weight exhibited the best synergistic effect on NGH inhibition in the methane-water system. Besides, earlier compounding work indicated that the inhibition capability of KHIs could be elevated by the addition of quaternary ammonium salts [26,27]. In recent years, the combination application of hydrate AAs and THIs also raised great interests. York and Firoozabadi [28] found that the performance of hydrate AAs (rhamnolipid and dicetyldimethylammonium chloride) can be improved by adding alcohol as cosurfactant. Methanol at the dosage of 0.5 wt% could help inhibit the hydrate agglomeration when the used hydrate AAs alone are ineffective. The synergistic inhibition performance of methanol and rhamnolipid on the NGH agglomeration in the cyclopentane/water/THF system was further discussed by Li et al. [29], and the analysis demonstrated that the addition of methanol could reduce the required concentration of rhamnolipid. Sun et al. [30] investigated the synergistic inhibition performance of various alcohols with rhamnolipid on agglomeration, and iso-propanol was screened as the most effective cosurfactant. Dong et al. [22] revealed the compounding performance of the hydrate AA (cocamidopropyl dimethylamine) and salt (NaCl). Results showed that the salt may make the AA ineffective at a very low water cut of only 10 %, while the water cut ranges from 30 % to 100 %, the AA of 1 wt% works if there is NaCl (salt) in the aqueous component due to the lowered water to hydrate conversion. Pei et al. [31] experimentally investigated the performance of developed hydrate AA + monoethylene glycol (MEG) on hydrate anti-agglomeration by using a gas flow pipe. Analysis demonstrated that hydrate AA and MEG exhibited a dual effect of antagonist and synergy when combined at the different proportion. At the optimal proportion of AA (0.01–0.025 wt%): MEG (10 wt%), the formation of NGH blockage may be retarded and the performance of hydrate AA + MEG is better than that of single inhibitor.

The field application of hydrate AAs has been reported, where the combined use of hydrate AAs and THIs was adopted for the transition from single application of THIs to hydrate AAs [32]. Therefore, clarification on the performance of hydrate AAs compounded THIs is of great significance. In this work, the typical candidate for THIs and hydrate AAs were selected as monoethylene glycol (MEG) and three kinds of QASs, respectively. Then, the performance of three kinds of QAS surfactants compounded with MEG are evaluated by a rocking apparatus. This research could provide a comprehensive understanding for the aspect of the hydrate control method with QAS + MEG hybrid inhibitors.

2. Experimental section

2.1. Materials

As for the employed materials, deionized water was used for hydrate formation. The deionized water (18.2 MΩ cm) was lab-made

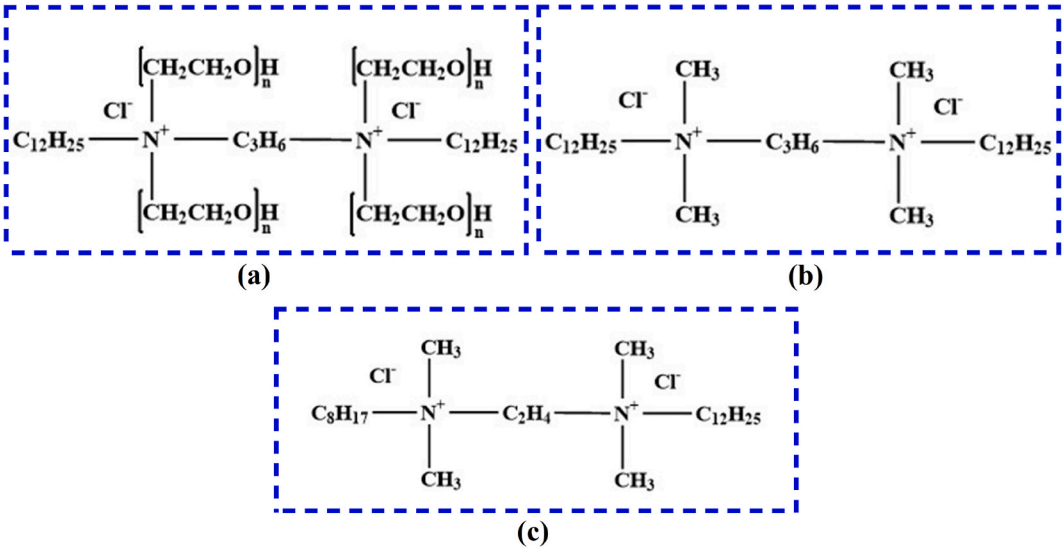

Fig. 1. Chemical formulas of the adopted QASs, including the AA-1 (a), AA-2 (b) and AA-3 (c).

Table 1
Codes and names of chemicals applied in the experiments.

Code	Reagent
AA-1	N^1,N^1,N^3,N^3-tetrapolyoxyethylene-N^1,N^3-didodecylpropane-1,3-diaminium chloride
AA-2	N^1,N^3-didodecyl-N^1,N^1,N^3,N^3-tetramethylpropane-1,3-diaminium chloride
AA-3	N^1-dodecy-N^1,N^1,N^2,N^2-tetramethyl-N^2-octylethane-1,2-diaminium chloride
MEG	Monoethylene glycol

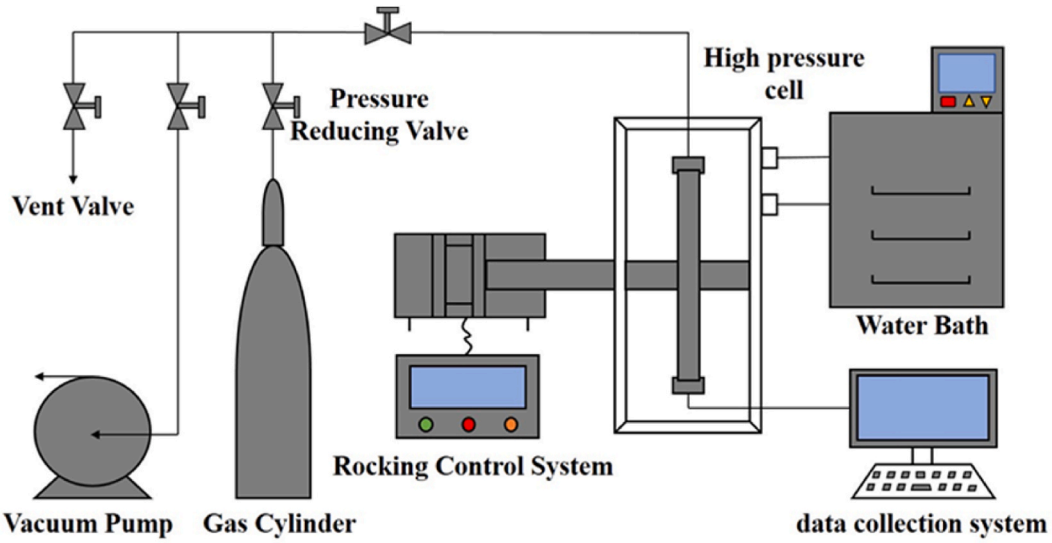

Fig. 2. Schematic of the high pressure rocking cell apparatus.

by using the deionized equipment in the laboratory. #5 mineral oil was purchased from Morunke Company. As described by the supplier, the density of #5 mineral oil is 0.82 g/cm^3 and the kinematic viscosity is 5.06 mm^2/s at 40 °C. Methane gas was purchased from Qingdao Xinkeyuan Gas Co., Ltd. MEG was purchased from Shanghai Aladdin Reagent Co., Ltd. QAS surfactants were purchased from Zhengzhou Yihe Fine Chemicals Co., Ltd: AA-1 (N^1,N^1,N^3,N^3-tetrapolyoxyethylene-N^1,N^3-didodecylpropane-1,3-diaminium chloride), AA-2 (N^1,N^3-didodecyl-N^1,N^1,N^3,N^3-tetramethylpropane-1,3-diaminium chloride), AA-3 (N^1-dodecy-N^1,N^1,N^2,N^2-tetramethyl-N^2-octylethane-1,2-diaminium chloride). The chemical formulas of the adopted salts are given in Fig. 1. The purchased

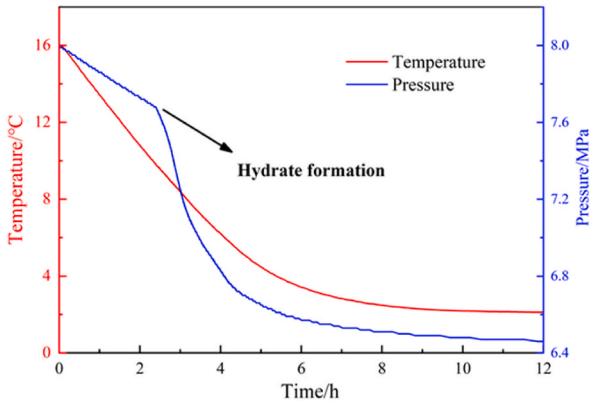

Fig. 3. Variation of temperature and pressure with time during the cooling process for the no-inhibitor system.

chemicals are directly applied without any further treatment. Detailed information of the chemicals is shown in Table 1.

2.2. Apparatus and procedures

A rocking cell apparatus was designed to test the inhibition capability of hydrate inhibitors at high methane pressure. The schematic of the employed rocking apparatus is present in Fig. 2. Overall, the apparatus consists of the rocking control system, rocking cell and data acquisition system. The rocking control system was used to control the rocking frequency as well as the preset angle of the high-pressure cell. The high-pressure cell is fixed to a rotating rod driven by a stepper motor. Temperature and pressure transducer are employed to monitor the pressure as well as temperature data in the cell. The slider inside the cell was designed as a combined section of PEEK plastic and stainless steel, where the inside positioner could be successfully monitored by a position sensor. During the rocking process, the trajectory of slider can be recorded by the data acquisition system. The effective inside volume of the high-pressure cell is 150 mL, and the maximum allowable pressure is 30 MPa. A water chiller (THX-2030H, Ningbo Tianheng) is used to keep the cell temperature as a constant value. The agglomeration of hydrate in the cell can be detected by monitoring the slider trajectories in the cell. If the hydrate agglomeration occurs, the movement of slider will be retarded. The detecting range of employed temperature transducer is −50 °C–100 °C, and the measuring range of pressure transducer is 0–40 MPa. For the oil-water system in this work, the slider could move in the full trajectory range of 7–200 mm without the hydrate formation.

The experimental procedure of this work is as follows:

(1) Firstly, the cell was cleaned for three times by using the deionized water and then wiped for dewatering;
(2) A preset volume of #5 mineral oil (70 mL), deionized water (30 mL) and chemical reagent (2 wt% QAS, 5–20 wt% MEG, based on the water mass) were preliminary mixed by using a glass rod. Then the mixture was transferred to the cell, and then the cell was sealed. After sealing, vacuum operations were performed on the cell to −0.1 MPa for the sufficient air removal. The liquid loading in the cell is 66.7 % (v/v) to 70.7 % (v/v), the water cut is 30 % (v/v).
(3) The gas injection valve was turned on to inject methane gas to the cell until reaching a certain pressure (8 MPa). Then the water bath temperature was constantly preset to be 16 °C;
(4) The rocking process was started to speed up the dissolution of gas. The set angle of rocking is 0–180°, and the set frequency of rocking is 3 times/min. At the same time, the oil, water and chemicals were further mixed during the rocking process. After the pressure decreased to a stable value, the methane gas injection was carried out to the cell until the cell pressure stabilized to a desired pressure. The slider trajectory, pressure and temperature data could be acquired with a data acquisition system;
(5) The water bath temperature was finally kept to be 0 °C, and the cell was cooled at a cooling speed of ~2 °C/h. The formation of NGH will occur during the cooling process. The variation of cell pressure and temperature during the NGH formation process is present in Fig. 3. In the cooling process, the cell pressure first slowly decreased with the reduced temperature, and the varying pressure together with temperature at this stage obeys the equation of state. Over a duration of ~4.2 h, the formation of NGH led to the rapid reduced pressure value. Finally, the hydrate formation rate slowed down with the consumption of methane gas, and the cell pressure tends to be stabilized. After the hydrate formation process has proceeded for sufficient time (~12 h), the hydrate dissociation was started. The water bath temperature was elevated to 16 °C for dissociating the hydrate in the cell.

2.3. Calculation on hydrate volume fraction

Quantifying the hydrate volume fraction in the cell is crucial to know the hydrate state. With the increase of hydrate volume fraction, the collision of NGH particles may be enhanced, which may promote the agglomeration of hydrate. Therefore, the determined volume fraction of NGH could significantly affect the flow ability of obtained NGH slurry.

In this way, the hydrate volume fraction should be accurately determined to characterize the inhibition capability of MEG + QAS

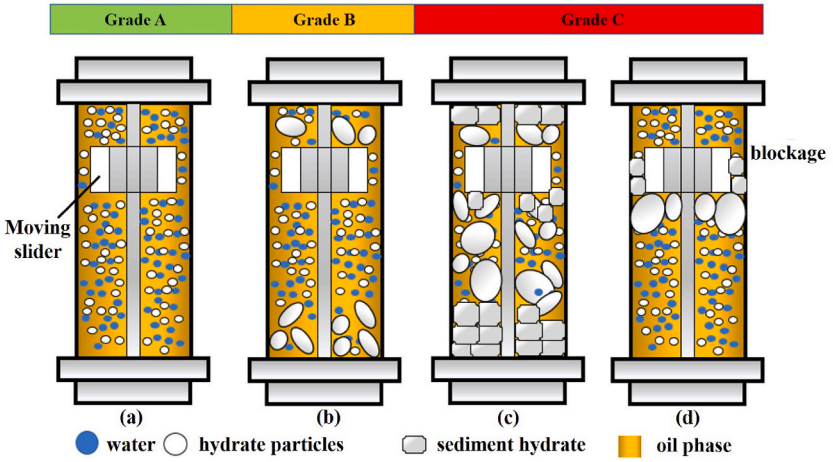

Fig. 4. Schematic of the classification for hydrate anti-agglomeration performance, including the grade A (a), grade B (b) and grade C (c, d).

hybrid hydrate inhibitor. Then, at the known volume fraction of NGH, the anti-agglomerating performance of chemicals could be comprehensively analyzed on the basis of slider trajectories during the hydrate formation process. The volume fraction of NGH is determined from methane gas consumption. The methane amount inside the cell prior to hydrate formation n_1 is given by Eq. (1).

$$n_1 = \frac{P_1 V_1}{ZRT_1} \tag{1}$$

where P_1 denotes gas pressure prior to NGH formation, MPa; T_1 denotes temperature with no hydrate, K; V_1 denotes gas volume in cell, mL; Z denotes compressibility factor of methane at the known pressure/temperature, which is calculated by Patel-Teja equation of state, R denotes ideal gas constant, which is 8.314 J mol^{-1} K^{-1}.

The methane amount of gaseous state n_2 during the NGH formation process is given by Eq. (2):

$$n2 = \frac{P_2 V_2}{ZRT_2} \tag{2}$$

where P_2 is the gas pressure in NGH formation, MPa; T_2 denotes temperature during NGH formation process, K; V_2 denotes gas volume in the cell, mL.

The methane amount in gaseous state which is consumed by hydrate formation n_{gas} is given by Eq. (3):

$$n_{gas} = n_1 - n_2 \tag{3}$$

Herein, the hydration number is set as 6. Thereby the amount of hydrate as well as the consumed water can be calculated. The volume of NGH could be given by Eq. (4) as follows:

$$V_{hyd} = \frac{m_{hyd}}{\rho_{hyd}} \tag{4}$$

where m_{hyd} denotes hydrate mass, g; ρ_{hyd} denotes density of methane hydrate, 0.91 g cm^{-3}.

Then the volume fraction of NGH φ is given by Eq. (5):

$$\varphi = \frac{V_{hyd}}{V_{hyd} + V_{oil} + V_{water} - V_{water,conv}} \tag{5}$$

where V_{hyd} denotes volume of methane hydrate, mL; V_{oil} denotes oil volume, mL; V_{water} denotes water volume before NGH formation; $V_{water,\ conv}$ denotes the water volume which is converted to NGH, mL.

2.4. Classification of hydrate anti-agglomerants performance

According to the slider moving trajectory in rocking cell, the agglomerating state of hydrate inside the cell can be evaluated, and the inhibition capability of hydrate inhibitors could be divided into three grades. Schematic of the classification for inhibition capability on NGH agglomeration is present in Fig. 4. With the presence of the grade A hydrate inhibitor, a well dispersion of NGH particles in the liquid phase could be achieved, and the slider moves in the full trajectory range during the whole experimental runs. With the addition of grade B chemicals with moderate performance, the agglomeration of hydrate can be mitigated but can hardly be prevented. In this case, a small amount of agglomerated hydrate will deposit at one side or both sides of the cell, though partial hydrate can be suspended

Table 2
Summary of the experiments for the performance evaluation of QAS + MEG hybrid hydrate inhibitors.

QAS	MEG concentration /wt%	Hydrate formation time /h	Final hydrate volume fraction/%	Final slider moving range/mm	Grade
No AA	0	2.39	5.18	–	C
No AA	5	4.24	10.66	–	C
No AA	10	4.94	9.87	88–153	B
No AA	20	5.44	8.34	11–190	B
AA-1	0	2.6	21.44	76–151	B
AA-1	5	3.71	16.12	7–200	A
AA-1	10	4.42	12.4	23–200	B
AA-1	20	6.23	8.52	7–200	A
AA-2	0	2.56	21.94	61–174	B
AA-2	5	4.03	13.64	8–190	B
AA-2	10	5.28	11.96	7–200	A
AA-2	20	5.1	9	7–200	A
AA-3	0	2.75	20.72	73–152	B
AA-3	5	4.19	15.94	61–177	B
AA-3	10	4.32	13.3	12–200	B
AA-3	20	5.37	9.74	7–200	A

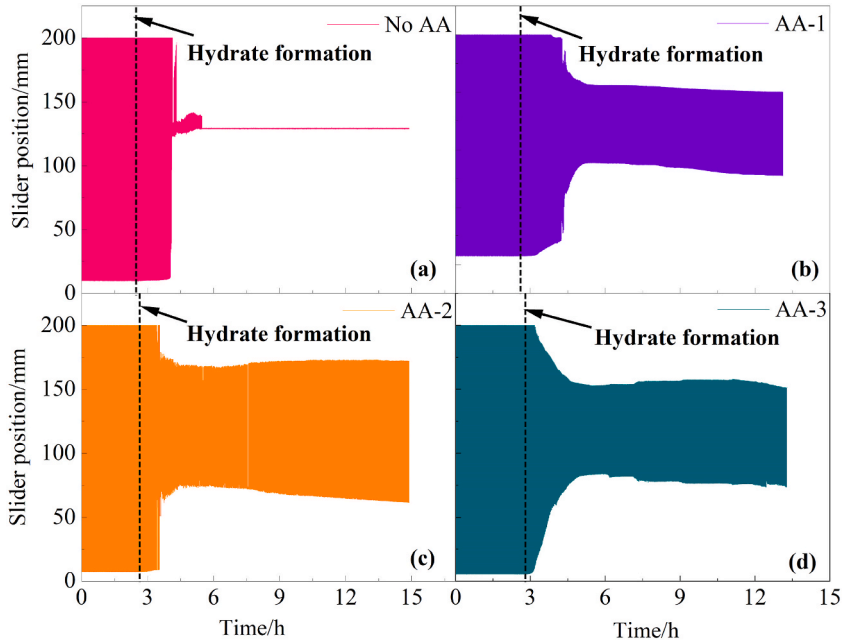

Fig. 5. Slider trajectories verse time in oil-water system during the hydrate formation process with no inhibitor and the presence of different QAS: no AA (a), AA-1 (b), AA-2 (c), AA-3 (d).

in liquid. Therefore, the range of slider trajectories will be reduced. By the end of hydrate formation process, the slider moves only inside a decreased trajectory range than grade A chemical. For the system with grade C chemical, the hydrate particles significantly agglomerate then deposit on the wall or the cell bottom due to the poor performance. As a consequence, the slider will be stuck at the fixed position in the cell during the rocking process.

3. Results and discussion

Under an initial pressure of 8 MPa and a water cut of 30 %, the performance of three QAS surfactants of 2 wt% (based on water) on hydrate agglomeration were evaluated. Subsequently, the adopted QAS were compounded with 0, 5, 10, and 20 wt% MEG for the performance evaluation of hydrate inhibitors, respectively. A total of 16 runs of experiments were conducted, which are shown in Table 2.

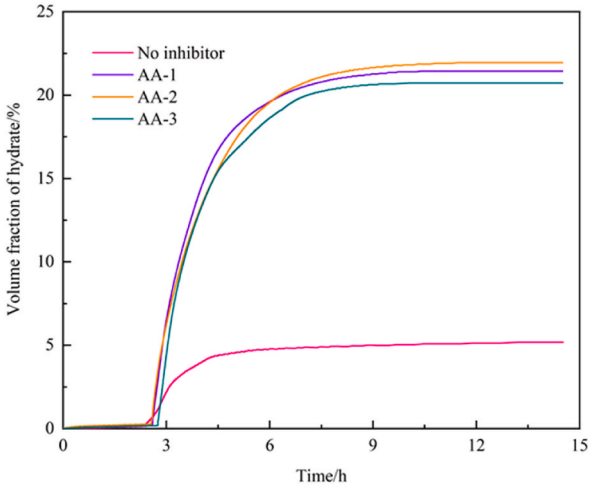

Fig. 6. Variation of hydrate volume fraction with time in oil-water system during the hydrate formation process with no inhibitor and the presence of different QAS.

3.1. Anti-agglomerating performance of QAS surfactants

In this work, the anti-agglomerating performance of three QASs were firstly experimentally evaluated. As is introduced in section 2.4, the anti-agglomerating performance of QASs was comprehensively analyzed on the basis of slider trajectory range together with calculated hydrate volume fraction. Prior to the inhibition capability test and compounding operations in this study, massive experiments have been carried out to choose good hydrate AAs among the commercial surfactants. As a result, these three gemini QASs were found to be with good hydrate anti-agglomerating performance. According to the literature, several gemini QASs have been found with excellent capability as good AAs compared to mono-QAS [13]. Herein, the three chosen gemini QASs also exhibited good hydrate anti-agglomeration performance. Fig. 5 presents the slider trajectories verse time in oil-water system in the NGH formation process with no additive and the presence of different QASs. The change of hydrate volume fraction versus time in water-oil system in the NGH formation process with no inhibitor additive and the presence of different QASs is shown in Fig. 6. During the cooling process, the NGH formation was started from the water droplet interface at the favorable temperature and pressure. Then the hydrate flakes spread to form hydrate shell. Upon the early formation stage, the NGH shell may be well suspended in liquid. Thus, the slider trajectory range was not be lowered with the NGH formation, and quite little difference was detected for the slider trajectory range at the early stage of NGH formation. Subsequently, the agglomerating of NGH happened because of the significant attraction between hydrate particles. The agglomerated hydrate may adhere on the inside wall or the slider surface, and led to the reduction of slider movement. Results showed that the slider could get stuck at a certain constant position when the hydrate volume fraction is only 5.18 %. Compared with the QAS containing system, the final volume fraction of NGH in no inhibitor situation is much lower than that of QAS system, which may be attributed to the mass transfer barrier by formation of hydrate plug. For the system with the addition of QAS, it can be seen that the volume fraction of NGH significantly increased with respect to the no inhibitor system. The final volume fraction of NGH in the AA-1, AA-2 and AA-3 containing system was found to be 21.44 %, 21.94 % and 20.72 %, respectively. According to the slider trajectory data, the AA-2 QAS has the best hydrate anti-agglomerating performance. The slider moved in a large trajectory range in the cell. Yet, the agglomerating of NGH can hardly be eliminated by using single QAS. There are still some agglomerated NGH deposition at the bottom side of cell, causing the reduction of slider trajectory range. Therefore, the adopted three QAS all exhibited the grade B performance. For the four runs of experiments, the addition of QAS was found to be with little influence on the onset of NGH formation, and the rapid NGH formation was observed after 2.39–2.75 h. In general, the hydrate anti-agglomerants mainly work by establishing steric repulsions among NGH particles. The functional groups (both hydrophilic and the lipophilic) of hydrate AAs cause the dual affinity to the NGH and oil. Upon the onset NGH formation, the hydrophilic head group adsorbs on the NGH surface, reversing the wettability of NGH surface. Therefore, a net repulsion situation among the NGH particles is obtained based on the resisting force of the lipophilic tails in oil. For the adopted gemini QASs in this work, the double ammonium ions are the basic hydrophilic head groups and the lipophilic tails tend to be hydrocarbon chain groups with more than 12 carbon atoms. Overall, the inhibition capability of adopted AAs on agglomerating is similar. The slightly different performance of the AAs may be attributed to the difference of the tail groups.

To verify this speculation, extra experimental runs were performed to characterize the stability of the water-oil dispersion. Herein, the mixture in the rocking apparatus was gathered after the 12-h rocking process for the evaluation of the emulsion effect. Macroscopically and microscopically, the images of the water-oil mixture in the no inhibitor system and the system in presence of hydrate AAs are present in Fig. 7. The microscopic pictures were acquired via the optical microscope apparatus (AOSVI W2-AF850) by preparing layered water-oil mixture using a glass slide. Based on the macroscopic observation (Fig. 7a–d), it can be seen that oil and water stratified for the no-inhibitor system. The necessity of emulsion should depend on the type of AAs. With the addition of surfactants,

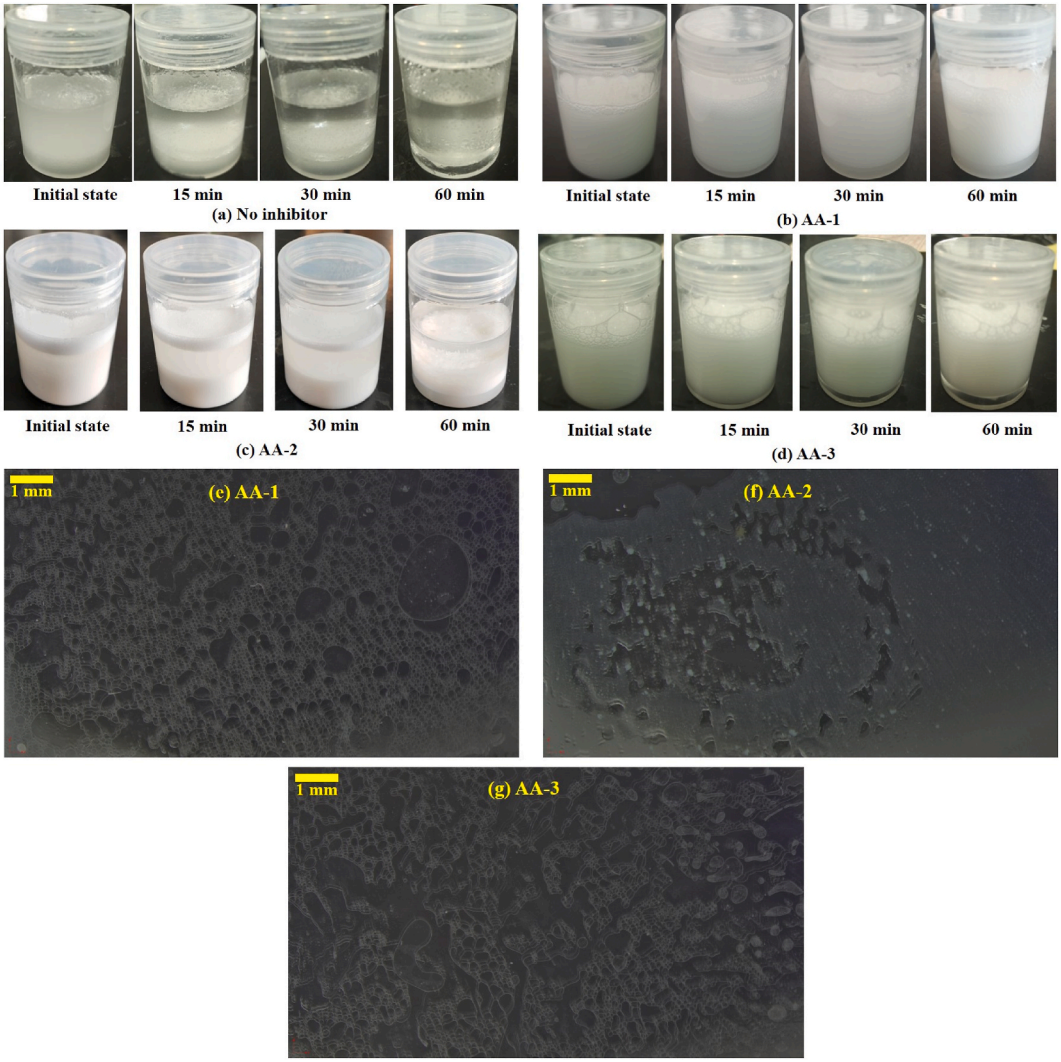

Fig. 7. The macroscopic (a–d) and microscopic image (e–g) of the oil-water mixture after the 12-h rocking process.

emulsions (initial state) were observed for the system with adding the AA-1 and AA-3, whereas merely partial emulsification was observed in the system with the AA-2. As the duration increased, the water and oil separated for all the system. The macroscopic images (Fig. 7e–g) showed that the emulsification effect of AA-1 and AA-3 is better than that of AA-2. However, the inhibition capability of adopted hydrate AAs is similar. Based on the results, good emulsification may do not ensure an excellent AA capability. Dating back to the late 1980s, a polymeric AA proposed by French Petroleum Institute is capable of emulsifying the total water in oil [6]. The formed NGH can be limited only inside the well-emulsified water droplets, thereby a good inhibition capability on agglomerating was obtained. The mechanism of the agglomerating inhibition capability was initially suggested to be emulsifying effect. Yet with the proceeding investigations, surfactants of excellent emulsifier may have a very poor inhibition capability on agglomerating, and the emulsifying effect was confirmed not correlated with anti-agglomerating capability [33–35].

3.2. Effect of MEG to AA-1 QAS

The AA-1 QAS was firstly compounded with MEG of different concentrations to evaluate the performance of the MEG + QAS hybrid hydrate inhibitor. Fig. 8 presents the slider trajectories verse time in oil-water system in the NGH formation period with the adding of AA-1 as well as MEG of different concentrations. The change of volume fraction of NGH verse time in water-oil system with AA-1 compounded with MEG of various concentrations is present in Fig. 9. According to the slider trajectories, it can be seen that the adding of MEG could significantly elevate the flow ability of NGH slurry, and the slider can migrate within a larger trajectory range. With the addition of 5 wt% MEG to the AA-1 QAS system, the slider trajectory range was found to be increased to 7–200 mm from 76 to 151 mm, resulting in the grade A performance. However, as the concentration of MEG was elevated to 10 wt%, the slider trajectory range was found to be reduced at the late stage of hydrate formation process, which indicated that there is small amount of hydrate

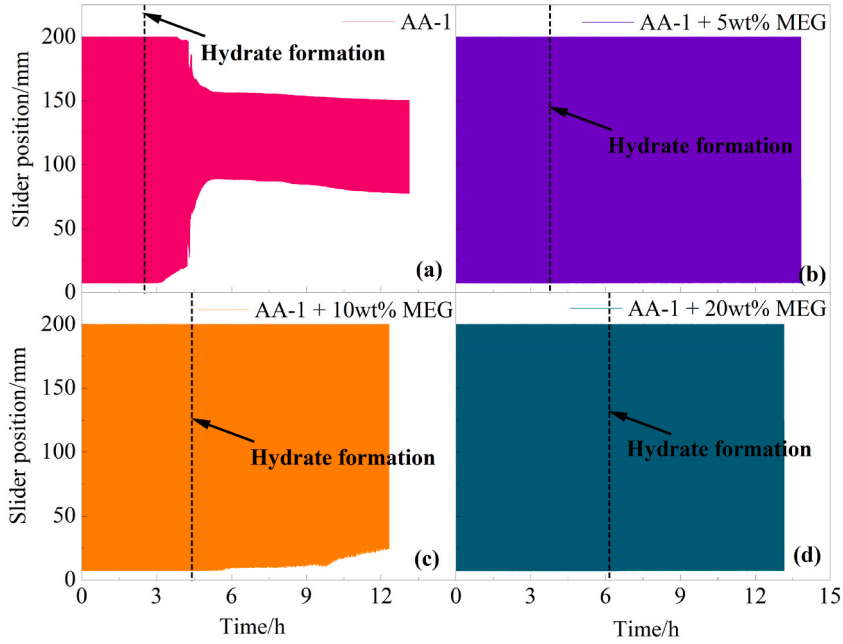

Fig. 8. Slider trajectories verse time in oil-water system during the hydrate formation process with the presence of AA-1 and MEG of different concentrations: AA-1 (a), AA-1+ 5 wt% MEG (b), AA-1+ 10 wt% MEG (c), AA-1+ 20 wt% MEG (d).

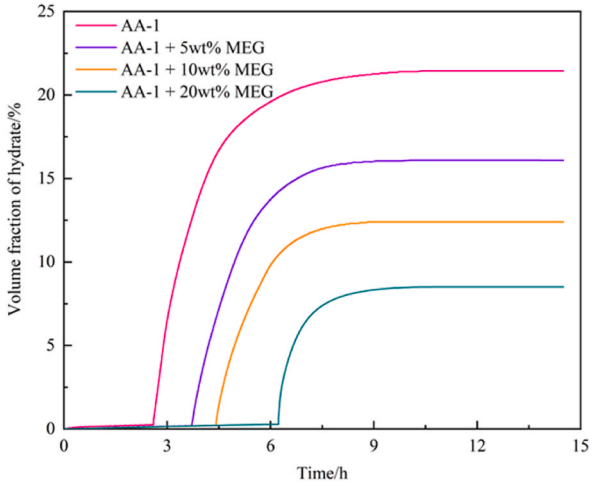

Fig. 9. Variation of hydrate volume fraction verse time in oil-water system with AA-1 compounded with MEG of different concentrations.

deposition on the cell bottom. Therefore, the performance of the AA-1+10 wt% MEG may be not stable at the high hydrate volume fraction. As the MEG concentration was elevated to 20 wt%, it was found that the slider could move freely within the whole range of the cell. The AA-1 + 20 wt% MEG compound exhibited the grade A performance. With the increasing MEG concentration, it can be found that the final volume fraction of NGH was significantly reduced. At the reduced volume fraction of NGH than the no MEG situation, the AA-1 QAS can effectively keep the hydrate dispersed in liquid phase. Thus, the flow ability of NGH slurry can be improved. Besides, the adding of MEG may also delay the onset of NGH formation process, because the increasing dosage of MEG moves the phase equilibrium conditions of NGH to a lower temperature at the same pressure, so that the subcooling degree for NGH formation in the MEG containing situation was reduced than the no MEG system. The phase equilibrium conditions of methane hydrate at the different MEG concentrations have been shown in Fig. 10 which is calculated by Multiflash software. According to the results calculated by Multiflash software, the structure of methane hydrate was determined as sI. It can be seen that the equilibrium pressure is much higher with the increase of MEG concentration at the same temperature, which is caused by the lowered water activity (inhibition effect of MEG). The equilibrium curves shifted to the left with the increase of MEG concentration. Due to the stronger inhibiting effect under the higher MEG concentration, the amount of formed hydrate in the cell will be reduced, which leads to the lower volume

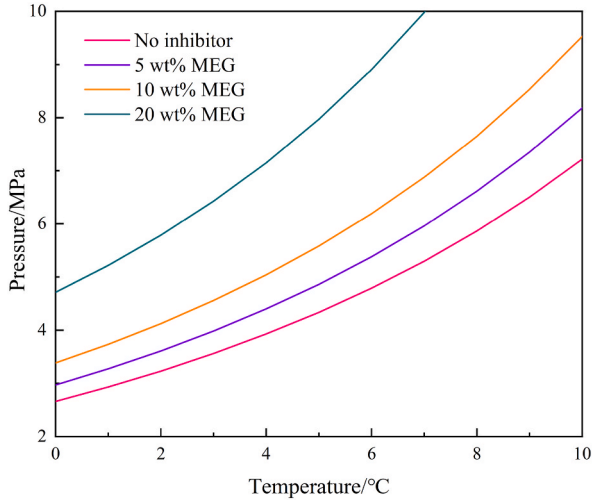

Fig. 10. Phase equilibrium conditions of methane hydrate at the different MEG concentrations.

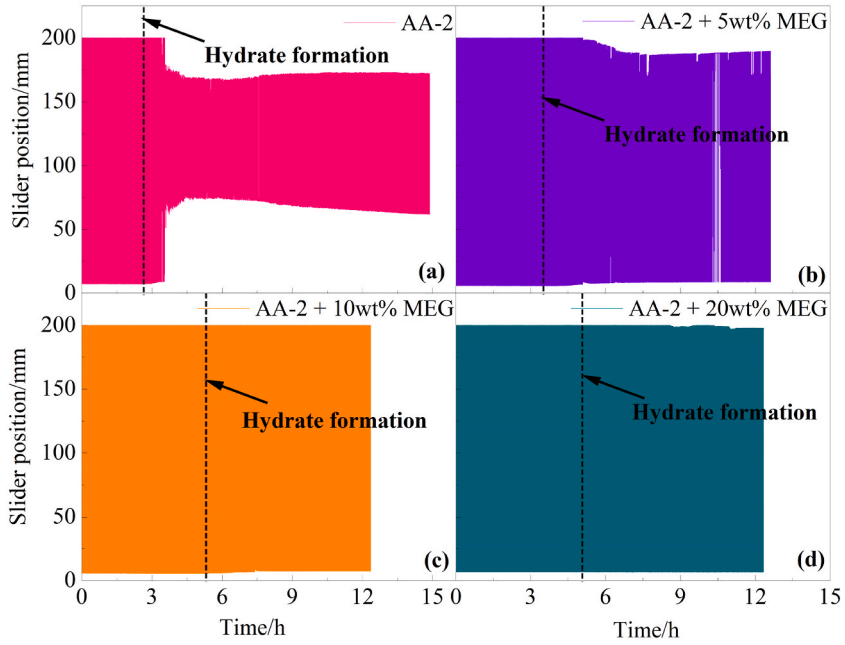

Fig. 11. Slider trajectories verse time in oil-water system during the hydrate formation process with the presence of AA-2 and MEG of different concentrations: AA-2 (a), AA-2+ 5 wt% MEG (b), AA-2+ 10 wt% MEG (c), AA-2+ 20 wt% MEG (d).

fraction of NGH. For the situation with no MEG, the limited slider trajectories (grade B performance) was mainly be caused by the high hydrate volume fraction, which is beyond the anti-agglomerating ability of hydrate AAs. For the AA + MEG system, at the reduced volume fraction of NGH, the hydrate AA can effectively keep the hydrate dispersed in liquid phase. Thus, the flow ability of NGH slurry can be improved. Besides, the adding of MEG could also delay the onset of NGH formation period, because the added MEG moves the phase equilibrium lines of NGH to a lower temperature at the same pressure, so that the subcooling degree for NGH formation in the MEG involving situation was reduced than the MEG free system. The NGH formation time was summarized in Table 2. The NGH formation time is much longer as the increase of MEG concentration, which may be attributed to the longer hydrate induction time by the lower subcooling degree for hydrate formation.

3.3. Effect of MEG to AA-2 QAS

The performance of AA-2 + MEG hybrid hydrate inhibitor was experimentally investigated. Fig. 11 shows the slider trajectories

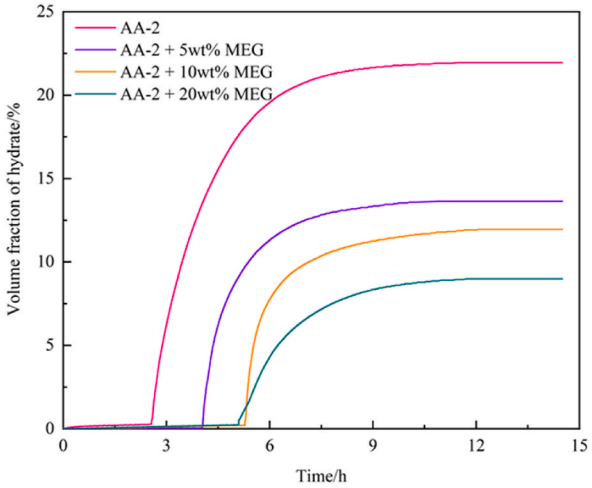

Fig. 12. Variation of hydrate volume fraction verse time in oil-water system with AA-2 compounded with MEG of different concentrations.

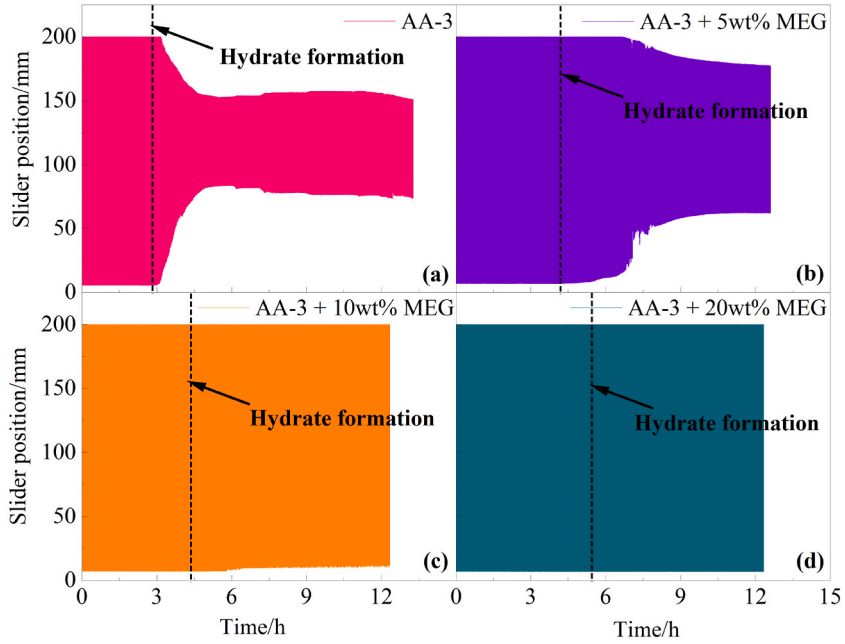

Fig. 13. Slider trajectories verse time in oil-water system during the hydrate formation process with the presence of AA-3 and MEG with different concentrations: AA-3 (a), AA-3+ 5 wt% MEG (b), AA-3+ 10 wt% MEG (c), AA-3+ 20 wt% MEG (d).

verse time in oil-water system in the NGH formation process with adding the AA-2 as well as MEG of different concentrations. The change of volume fraction of NGH verse time in water-oil system with AA-2 compounded with MEG of different concentrations is present in Fig. 12. In comparison with the AA-2 only situation, the addition of MEG can significantly delay the onset formation of NGH. Besides, at the reduced volume fraction of NGH, the AA-2 QAS can more effectively help inhibit the agglomerating of NGH particles in liquid. After adding the 5 wt% MEG to AA-2, the slider trajectory range increased from 61-174 mm to 8–190 mm, which means that less hydrate deposits at the cell bottom. The performance of AA-2+ 5 wt% MEG is classified to be grade B. Under the further increasing of MEG concentration to 10 wt% and 20 wt%, the slider moved in the full trajectory range, and the performance of the hybrid hydrate inhibitor was classified as grade A. The final hydrate volume fraction with the adding of 10 wt% or 20 wt% MEG is much lower. When the MEG concentration reaches 20 wt%, the final volume fraction of NGH was only 9 %. Under the limited volume fraction of NGH, the AA-2 can make the NGH particles well suspended in liquid. Thus, the addition of MEG has a synergy capability on improving the flow ability of NGH slurry.

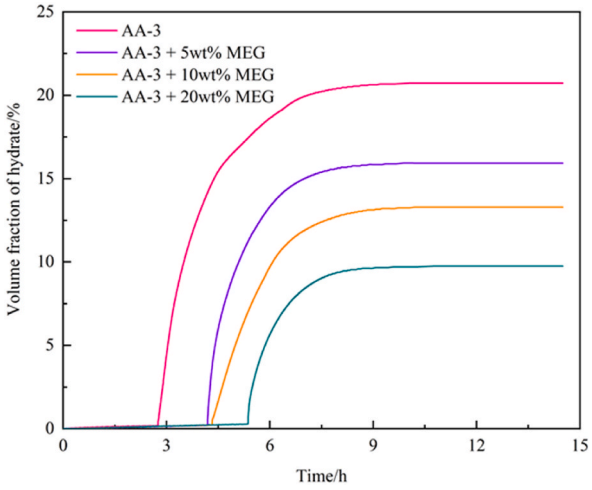

Fig. 14. Variation of hydrate volume fraction verse time in oil-water system with AA-3 compounded with MEG of different concentrations.

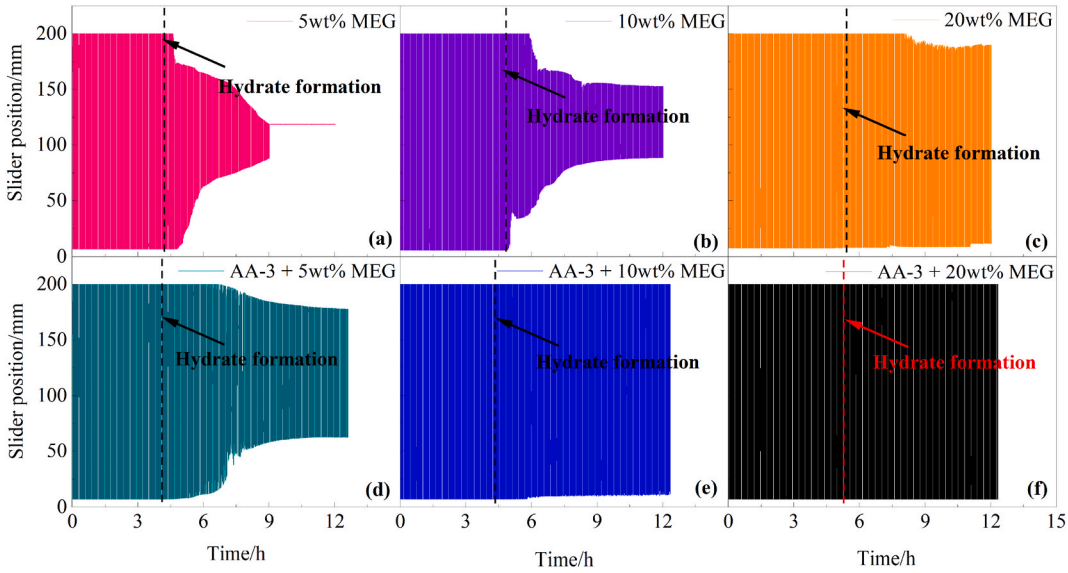

Fig. 15. Comparison on slider trajectories in MEG containing oil-water system with and without AA-3: 5 wt% MEG (a), 10 wt% MEG (b), 20 wt% MEG (c), AA-3 + 5 wt% MEG (d), AA-3 + 10 wt% MEG (e), AA-3 + 20 wt% MEG (f).

3.4. Effect of MEG to AA-3 QAS

In this work, the synergy effect of MEG to AA-3 QAS was experimentally evaluated. Fig. 13 shows the slider trajectories verse time in oil-water system in the NGH formation period with the adding of AA-3 and MEG with different concentrations. The changes of volume fraction of NGH verse time in water-oil system with AA-3 compounded with MEG of various concentrations are present in Fig. 14. Similar with the AA-2 + MEG system, the adding of MEG can also significantly delay the onset formation of NGH compared with the AA-3 only system. The slider trajectory range increased from 73-152 mm to 61–177 mm, indicating that less hydrate deposits at the cell bottom. The performance of the AA-3 + 5 wt% MEG is classified as grade B. When the MEG concentration increased to 10 wt % or further 20 wt%, the performance of AA-3 + MEG hybrid hydrate inhibitor can be significantly improved to grade A. The slider moved at a full trajectory range, which indicates that the NGH particles are well suspended and no agglomeration occurred. When the MEG concentration is 10 wt%, the slider moving range is 12–200 mm, and the final volume fraction of NGH is 13.3 %. In this situation, there is very little amount of hydrate deposits at the cell bottom. In general, the synergy effect of MEG to the QAS on the flow ability of NGH slurry could be attributed to two reasons. First, the addition of MEG can move the phase boundary of NGH to a lower temperature at the same pressure, thereby delay the onset formation of NGH and lower the final volume fraction of NGH. At the reduced hydrate volume fraction, QAS could be adsorbed on the NGH surface to form the spatial repulsion between NGH particles and prevent the NGH

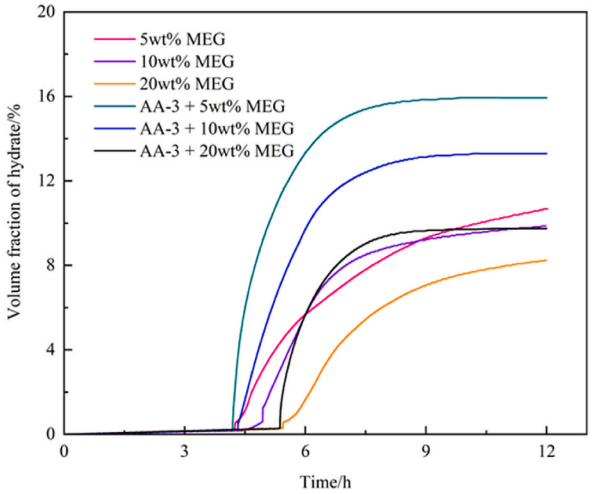

Fig. 16. Comparison on hydrate volume fraction change in MEG containing oil-water system with and without AA-3.

agglomeration. The MEG + QAS hybrid hydrate inhibitor could be a promising option for hydrate management.

3.5. *Effect of AA-3 QAS to MEG*

According to the above mentioned results, the hydrate anti-agglomeration performance of QAS + MEG hybrid hydrate inhibitor is much better than that of single QAS. With the adding of MEG, the volume fraction of NGH can be reduced, at which the agglomeration of NGH could be mitigated with QAS. Herein, to further distinguish the capability of hydrate AA, comparisons on slider trajectories and volume fraction of NGH in MEG containing water-oil system with and without AA-3 were conducted, which are shown in Figs. 15 and 16, respectively. For the MEG only system, the hydrate plug occurred in the 5 wt% MEG situation, which was caused by the uninhibited agglomerating of NGH particles. The slider finally got stuck at a constant position. The performance of single 5 wt% MEG is grade C. As the increasing of MEG concentration to 10 wt%, the final volume fraction of NGH decreased from 10.66 % to 9.87 %. At the same time, the slider moved at a decreased trajectory range instead of getting stuck at a certain position. As the MEG concentration further increased to 20 wt%, the slider moved at the almost full moving range. At the corresponding NGH volume fraction, the well suspension of NGH particles can be obtained. The 10 wt% and 20 wt% MEG exhibited the grade B performance. However, it can be seen that the performance of QAS + MEG is much better than that of single MEG. The hybrid hydrate inhibitor of 2 wt% AA-3 + 10 wt% MEG and 2 wt% AA-3 + 20 wt% MEG exhibited the grade A performance. The flow ability of NGH was improved by the addition of QAS even if at a higher NGH volume fraction than the MEG only system, and the range of slider trajectory significantly increased. Therefore, the combined use of MEG and QAS has a good application prospect. For the achievement of NGH slurry at the same flow characteristics, the addition of QAS can reduce the usage of thermodynamic inhibitors (MEG), thereby further reduce the total costs for hydrate management.

4. Conclusions

In this work, the anti-agglomerating performance for NGH of three QAS was evaluated by using the high-pressure rocking cell, then the three QAS were compounded with MEG of the different concentrations, respectively. Some conclusions can be drawn as follows:

(1) The adopted three QAS are found with hydrate anti-agglomerating performance. Among the three QAS, the performance of AA-2 (N^1,N^3-didodecyl-N^1,N^1,N^3,N^3-tetramethylpropane-1,3-diaminium chloride) is the best. However, the agglomeration of hydrate can hardly be eliminated by using single QAS;
(2) The compounding performance of three QASs and MEG was investigated. It was found that the synergistic effect of AA-1 (N^1,N^1,N^3,N^3-tetrapolyoxyethylene-N^1,N^3-didodecylpropane-1,3-diaminium chloride) and 5 wt% MEG can completely prevent hydrate agglomeration;
(3) The combined use of QAS + MEG can effectively mitigate hydrate agglomeration, and the usage of can be significantly reduced. The MEG + QAS hybrid hydrate inhibitor could be a promising option for hydrate management.

Data availability statement

Data associated with the study has not been deposited into a publicly available repository. Data included in article/supp. material/referenced in article. The further inquiries on the original data in this study can be directed to the corresponding author.

Additional information

No additional information is available for this paper.

CRediT authorship contribution statement

Qibin Zhao: Writing – original draft, Investigation, Formal analysis, Conceptualization. **Hao Liang:** Writing – review & editing, Writing – original draft, Investigation, Formal analysis, Conceptualization.

Declaration of competing interest

The authors declare that they have no known competing financial interests or personal relationships that could have appeared to influence the work reported in this paper.

Acknowledgments

This work was financially supported by the CNOOC R&D project (CCL2021HNFN0209). The authors thank Dr. Litao Chen in China University of Petroleum (East China) for providing the rocking cell apparatus and useful discussions. The authors thank Mr. Jiakai Ji and Mr. Zhijie Liao for their help in experiments.

References

[1] E.D. Sloan, C.A. Koh, Clathrate Hydrates of Natural Gases, third ed., CRC Press, Boca Raton, FL, USA, 2008, pp. 1–9.
[2] E.D. Sloan, C.A. Koh, A.K. Sum, Natural Gas Hydrates in Flow Assurance, Gulf Professional Publishing, Oxford, 2010, pp. 37–47.
[3] W. Liu, M. Zhang, Z. Liu, C. Lang, J. Lu, Q. Li, Y. Li, Investigation on hydrate formation and viscosity of the gas–water system in Lingshui gas field of South China Sea, Energy Fuel. 27 (2023) 2833–2842, https://doi.org/10.1021/acs.energyfuels.2c04009.
[4] S.K. Nagappayya, R.M. Lucente-Schultz, V.M. Nace, V.M. Ho, Antiagglomerant hydrate inhibitors: the link between hydratephilic surfactant behavior and inhibition performance, J. Chem. Eng. Data 60 (2015) 351–355, https://doi.org/10.1021/je500611d.
[5] A. Hassanpouryouzband, E. Joonaki, M.V. Farahani, S. Takeya, C. Ruppel, J. Yang, N.J. English, J.M. Schicks, K. Edlmann, H. Mehrabian, Z.A. Aman, B. Tohidi, Gas hydrates in sustainable chemistry, Chem. Soc. Rev. 49 (2020) 5225–5309, https://doi.org/10.1039/c8cs00989a.
[6] M.A. Kelland, History of the development of low dosage hydrate inhibitors, Energy Fuel. 20 (2006) 825–847, https://doi.org/10.1021/ef050427x.
[7] L. Zhen, X.B. Zhou, Z.L. Lu, D.Q. Liang, Kinetic inhibition performance of N-vinyl caprolactam/isopropylacrylamide copolymers on methane hydrate formation, Energy 242 (2022) 123056, https://doi.org/10.1016/j.energy.2021.123056.
[8] S.P. Kang, D. Lee, J.W. Lee, Anti-agglomeration effects of biodegradable surfactants from natural sources on natural gas hydrate formation, Energies 13 (2020) 1107, https://doi.org/10.3390/en13051107.
[9] M.W. Sun, A. Firoozabadi, New surfactant for hydrate anti-agglomeration in hydrocarbon flowlines and seabed oil capture, J. Colloid Interface Sci. 402 (2013) 312–319, https://doi.org/10.1016/j.jcis.2013.02.053.
[10] U.C. Klomp, V.R. Kruka, V.R. Reijnhart, A.J. Weisenborn, Method for inhibiting the plugging of conduits by gas hydrates, US Patent WO 93/25798 (1993).
[11] H. Delroisse, J.P. Torre, C. Dicharry, Effects of a quaternary ammonium salt on the growth, wettability, and agglomeration of structure II hydrate crystals, Energy Fuel. 32 (2018) 12277–12288, https://doi.org/10.1021/acs.energyfuels.8b02980.
[12] M.A. Kelland, Production Chemicals for the Oil and Gas Industry, second ed., CRC Press, Boca Raton, FL, 2014, pp. 375–396.
[13] A.K. Norland, M.A. Kelland, Crystal growth inhibition of tetrahydrofuran hydrate with bis- and polyquaternary ammonium salts, Chem. Eng. Sci. 69 (2012) 483–491, https://doi.org/10.1016/j.ces.2011.11.003.
[14] C.H. Yu, C. Yue, B.J. Sun, X. Yang, J.K. Ji, Z.L. Meng, L.T. Chen, Screening hydrate anti-agglomerants for an oil–gas–water system from various commercial chemicals using rocking cells, Energy Fuel. 36 (2022) 10685–10701, https://doi.org/10.1021/acs.energyfuels.2c01285.
[15] M.L. Zanota, C. Dicharry, A. Graciaa, Hydrate plug prevention by quaternary ammonium salts, Energy Fuel. 19 (2005) 584–590, https://doi.org/10.1021/ef040064l.
[16] C. Dicharry, H. Delroisse, J.P. Torre, G. Barreto, Using microscopic observations of cyclopentane hydrate crystal morphology and growth patterns to estimate the antiagglomeration capacity of surfactants, Energy Fuel. 34 (2020) 5176–5187, https://doi.org/10.1021/acs.energyfuels.9b03395.
[17] J.D. York, A. Firoozabadi, Comparing effectiveness of rhamnolipid biosurfactant with a quaternary ammonium salt surfactant for hydrate anti-agglomeration, J. Phys. Chem. B 112 (2008) 845–851, https://doi.org/10.1021/jp077271h.
[18] L.L. Shi, Y. He, J.S. Lu, G.D. Hou, D.Q. Liang, Anti-agglomeration evaluation and Raman spectroscopic analysis on mixed biosurfactants for preventing CH_4 hydrate blockage in n-octane plus water systems, Energy 229 (2021) 120755, https://doi.org/10.1016/j.energy.2021.120755.
[19] X.Q. Wang, H.B. Qin, Q.L. Ma, Z.F. Sun, K.L. Yan, Z.Y. Song, K. Guo, D.M. Liu, G.J. Chen, C.Y. Sun, Hydrate antiagglomeration performance for the active components extracted from a terrestrial plant fruit, Energy Fuel. 31 (2017) 287–298.
[20] K.L. Yan, C.Y. Sun, J. Chen, L.T. Chen, D.J. Shen, B. Liu, M.L. Jia, M. Niu, Y.N. Lv, N. Li, Z.Y. Song, S.S. Niu, G.J. Chen, Flow characteristics and rheological properties of natural gas hydrate slurry in the presence of anti-agglomerant in a flow loop apparatus, Chem. Eng. Sci. 106 (2014) 99–108, https://doi.org/10.1016/j.ces.2013.11.015.
[21] M.W. Sun, A. Firoozabadi, New Hydrate Anti-agglomerants Formulation for Offshore Flow Assurance and Oil Capture, Offshore Technology Conference, Houston, TX, 2014. OTC-25439-MS.
[22] S.B. Dong, A. Firoozabadi, Effect of salt and water cuts on hydrate anti-agglomeration in a gas condensate system at high pressure, Fuel 210 (2017) 713–720, https://doi.org/10.1016/j.fuel.2017.08.096.
[23] S.B. Dong, A. Firoozabadi, Hydrate anti-agglomeration and synergy effect in normal octane at varying water cuts and salt concentrations, J. Chem. Thermodyn. 117 (2018) 214–222, https://doi.org/10.1016/j.jct.2017.09.016.
[24] S.B. Dong, M.Z. Li, C.W. Liu, Study on the synergistic properties of two nonionic natural gas hydrate anti-agglomerants via rocking cell tests, Int. J. Energy Power Eng. 6 (2017) 84–90, https://doi.org/10.11648/j.ijepe.20170606.11.
[25] S. Foroutan, H. Mohsenzade, A. Dashti, H. Roosta, Comparison of kinetic inhibition of ethylene and methane hydrate formation when PEGs with low and high molecular weights meet common KHIs, Fuel 276 (2020) 118029, https://doi.org/10.1016/j.fuel.2020.118029.
[26] M.F. Mady, M.A. Kelland, Tris(tert-heptyl)-N-alkyl-1-ammonium bromides-powerful THF hydrate crystal growth inhibitors and their synergism with poly-vinylcaprolactam kinetic gas hydrate inhibitor, Chem. Eng. Sci. 144 (2016) 275–282, https://doi.org/10.1016/j.ces.2016.01.057.
[27] M.F. Mady, M.A. Kelland, Synergism oftert-heptylated quaternary ammonium salts with poly(N-vinyl caprolactam) kinetic hydrate inhibitor in high-pressure and oil-based systems, Energy Fuel. 32 (2018) 4841–4849, https://doi.org/10.1021/acs.energyfuels.8b00110.
[28] J.D. York, A. Firoozabadi, Alcohol cosurfactants in hydrate antiagglomeration, J. Phys. Chem. B 112 (2008) 10455–10465, https://doi.org/10.1021/jp8017265.

[29] X.K. Li, L. Negadi, A. Firoozabadi, Anti-agglomeration in cyclopentane hydrates from bio- and co-surfactants, Energy Fuel. 24 (2010) 4937–4943, https://doi.org/10.1021/ef100622p.
[30] M. Sun, Y. Wang, A. Firoozabadi, Effectiveness of alcohol cosurfactants in hydrate anti-agglomeration, Energy Fuel. 26 (2012) 5626–5632, https://doi.org/10.1021/ef300922h.
[31] J.H. Pei, Z.Y. Wang, P.F. Li, J.J. Hu, S.K. Tong, J. Zhong, P. Liu, W.Q. Fu, Experimental investigation on highly potent inhibitors of natural gas hydrate in oil-free flow system, Fuel 343 (2023) 127996, https://doi.org/10.1016/j.fuel.2023.127996.
[32] Z. Patel, M. Dibello, K. Fontentot, A. Guillory, R.M. Hesketh-Prichard, Continuous Application of Anti-agglomerant LDHI for Gas-Condensate Subsea Tieback Wells in Deepwater Gulf of Mexico, Offshore Technology Conference, Houston, TX, 2011. OTC-21836.
[33] Z. Huo, E. Freer, M. Lamar, B. Sannigrahi, D.M. Knauss, E.D. Sloan, Hydrate plug prevention by anti-agglomeration, Chem. Eng. Sci. 56 (2001) 4979–4991, https://doi.org/10.1016/S0009-2509(01)00188-9.
[34] M.A. Kelland, T.M. Svartaas, J. Ovsthus, T. Tomita, K. Mizuta, Studies on some alkylamide surfactant gas hydrate anti-agglomerants, Chem. Eng. Sci. 61 (2006) 4290–4298, https://doi.org/10.1016/j.ces.2006.02.016.
[35] O. Urdahl, A. Lund, P. Mork, T.N. Nilsen, Inhibition of gas hydrate formation by means of chemical additives - I. Development of an experimental set-up for characterization of gas hydrate inhibitor efficiency with respect to flow properties and deposition, Chem. Eng. Sci. 50 (1995) 863–870, https://doi.org/10.1016/0009-2509(94)00471-3.